JTE HCMUTE
ISSN: 2615-9740

JOURNAL OF TECHNICAL EDUCATION SCIENCE
Ho Chi Minh City University of Technology and Education
Website: https://jte.edu.vn
Email: jte@hcmute.edu.vn

Workspace Mapping and Force Control for the 3-DOF Robot

Tien Dat Nguyen, Phi Cuong Ly, Minh Khiem Tran, Duc Thien Tran*
HCMC University of Technology and Education (HCMUTE), Vietnam

*Corresponding author. *Email: thientd@hcmute.edu.vn*

ARTICLE INFO

Received: 29/07/2023
Revised: 01/10/2023
Accepted: 21/10/2023
Published: 28/04/2024

KEYWORDS

Workspace mapping;
Novint Falcon;
Teleoperation system;
Haptic rendering;
Haptic device.

ABSTRACT

This paper proposes a mapping method to unify two workspaces for the robot arm on the teleoperation system and apply the haptic method when the robot enters the singularity area. The teleoperation system mainly consists of a single master and a single slave. The master is a joystick device, and the slave is a 3-DOF manipulator. The master effectuates a setpoint signal to control the 3-DOF manipulator movement along a planned trajectory. Master and slave communicate via a wireless network. Due to differences in structure and dimensions, the workspaces of the master and slave are not analogous. Therefore, the Position mapping method is utilized to map two workspaces together. Otherwise, when the slave moves out of the limited space, the manipulator does not operate. The Haptic feedback is proposed to create the force, which reflects the palm of the operator. So the operator can feel and move to the permitted workspace. Several experiments have been implemented on the actual model to evaluate the effectiveness of the proposed system. The experimental results show the potential use of the teleoperation robotic system employing the Novint Falcon device, 3-DOF manipulator, and Position mapping method. This efficient mapping technique spans the slave workspace with high dexterity.

Doi: https://doi.org/10.54644/jte.2024.1435

1. Introduction

Nowadays, teleoperation systems are standard, especially in teleoperated robot control. These systems are highly needed for works of dangerous nature and dangerous working environments where humans cannot operate the robot directly. At present, the remote control system has broad application prospects in the industry, service, construction, medical care, and national defense [1], deep-sea operations [2], nuclear material treatment [3], and space exploration [4]. The teleoperation system consists of at least one master robot, controlled by the operator, and at least one slave robot that mimics the movements of the master robot via a wireless network to interact with the environment around. Besides, the structure types of the system, such as multi-master/single-slave, single-master/multi-slave, and multi-master/multi-slave. [5].

In the structure of the teleoperation system, the workspace of the master and slave has the same feature about shaping and sizing, which is convenient for controlling. However, the robot has many types of realistic, so their two workspaces are also dissimilar. Therefore, the problem of homogenizing the workspace of two robots is challenging and needs to be solved in the teleoperation system. Recently, most researchers have used a method to solve this problem called "Position Control." The experimental results show that the accuracy of the position is improved, but the factor must be investigated many times to choose the relevant factor for the robot. Otherwise, studying the advanced Position Control changes the Scaling value the following time [6]. This factor depends on the linear velocity of the end effector and gains stability. However, the active workspace of the robot is limited in the small space. This issue can be resolved by the Rate Control method [7], which shows the workspace expansion by adjusting the center of the chosen area to a new center on the workspace of the robot and is used by setting the velocity command of the slave robot proportional to the pose displacement of the master robot. Besides, the mapping methods such as Constant Scaling Control (CSC) and Variable Scaling Control (VSC) are optimal algorithms, but the VSC has a feature that overcomes the disadvantages of CSC. It is also applied to compare the advantages and disadvantages of each algorithm, besides in the

JTE
HCMUTE
ISSN: 2615-9740

JOURNAL OF TECHNICAL EDUCATION SCIENCE
Ho Chi Minh City University of Technology and Education
Website: https://jte.edu.vn
Email: jte@hcmute.edu.vn

application to control the slave surgical robot in teleoperation surgery [8] using a variation of Modified Rate Control. Otherwise, most researchers use the neuron network to combine the workspaces on the Ballistic system for trajectory planning [9]. In the articles [10], [11], two methods were proposed: rate control for coarse motion and a variable scaled position mapping for accurate positioning - to achieve efficient and precise teleoperation. However, the current implementation still requires manual switching between the mapping modes for sequential teleoperation tasks, which means that the teleoperation cannot be performed continuously. In Vietnam, most research involves designing an adaptive controller for a 3-DOF manipulator [12], [13]. However, mapping methods are limited in applying this robot's teleoperation system.

Through an analysis related to the teleoperation system, the Haptic method helps to increase the intuition of the operator when controlling the robot. Besides, a camera with force feedback can feel or interact with the object's shape in the environment [14]. To ensure system safety, we use Haptic feedback based on slave robot position displacement. One Hook law method improves precision [15]; the damping system is proposed to be stable when operating.

Related to the analyses mentioned above, this paper proposes a position mapping algorithm to convert the motion position of a joystick device into the workspace position of a slave robot. This conversion enhances the efficiency and accuracy of remote-control operations. The proposed approach incorporates a haptic feedback method to ensure the slave robot remains within the working area during the remote-control process. This allows for mapping the entire workspace of the control lever into the virtual workspace of the slave robot, thereby expanding the virtual workspace area compared to the mapping of a selected rectangular workspace. The proposed methods are applied to an experimental model consisting of one master device equipped with a Novint Falcon haptic device connected to a laptop and one slave device consisting of a 3-degree-of-freedom robot with three stepper motors controlled by Atmega2560 microcontrollers. A Zigbee wireless network is utilized for data exchange and communication between the master and slave devices. Through experimental results, the effectiveness of the position mapping method combined with haptic feedback is demonstrated.

The structure of this paper is organized as follows: the kinematics for the Haptic device and the 3-DOF robot in section 2. Section 3 presents the mapping and haptic methods for preventing control of the slave robot out of the workspace. Section 4 includes the result of the mapping and haptic method. Section 5 presented the conclusion of the proposed method.

2. Description of the teleoperation system

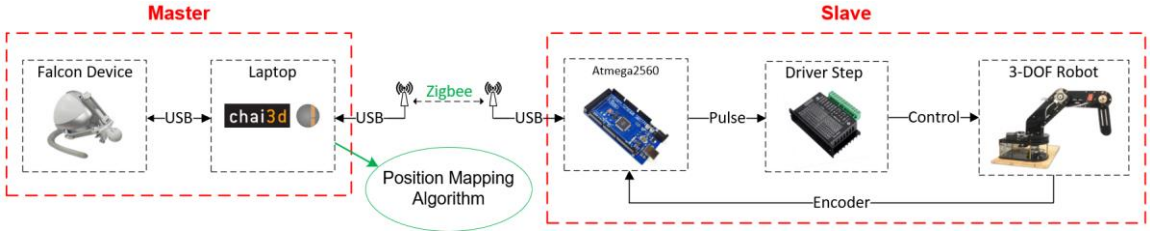

Figure 1. *Overview of the teleoperation system*

Figure 1 illustrates the overview of the master/slave teleoperation system. In detail, the Haptic Device block has position-sensing digital encoders that keep sending the position data at a frequency setup of 1kHz to the Laptop via USB. The laptop block receives data from the Haptic Device block through the CHAI3D software built to support communication with the Haptic Device lines. The position mapping algorithm is also built on the laptop. Zigbee wireless network is responsible for communication between Master and Slave at a baud rate speed of 115200. The Atmega2560 block is responsible for receiving the signal setpoint from the master; after calculating the kinematics for the robot, it proceeds to generate the pulse control drive step. Besides, there is also the task of reading the Encoder at the joints of the 3-DOF robot. The Driver Step block is responsible for controlling each stepper motor. The 3-DOF robot block is the actuator responsible for moving according to the control signal of the Driver step.

JTE HCMUTE
ISSN: 2615-9740
JOURNAL OF TECHNICAL EDUCATION SCIENCE
Ho Chi Minh City University of Technology and Education
Website: https://jte.edu.vn
Email: jte@hcmute.edu.vn

The structure of the joystick Novint Falcon is a parallel 3-DOF robot equipped with a sensor to measure the angle at the joint robot, a force sensor to help raise the sensing ability, and a button to adjust the model on the end effector [16]. Most of the research about the Novint Falcon is about forward and inverse kinematics. It identifies the parameters of the robot system by measuring the feedback signal at each joint [17], [18]. The slave robot is a 3-DOF robot whose mission is to track the desired signals from the joystick. The robot is equipped with 3 Encoders AMT322D-V with a revolution of 400 pulses/rev at each joint to read the angle position of the robot. Besides, the kinematics of the robot are calculated following the Denavit – Hartenberg (DH) method.

2.1. Kinematic of the haptic devices and 3-DOF robot

2.1.1. The inverse kinematic of the haptic device

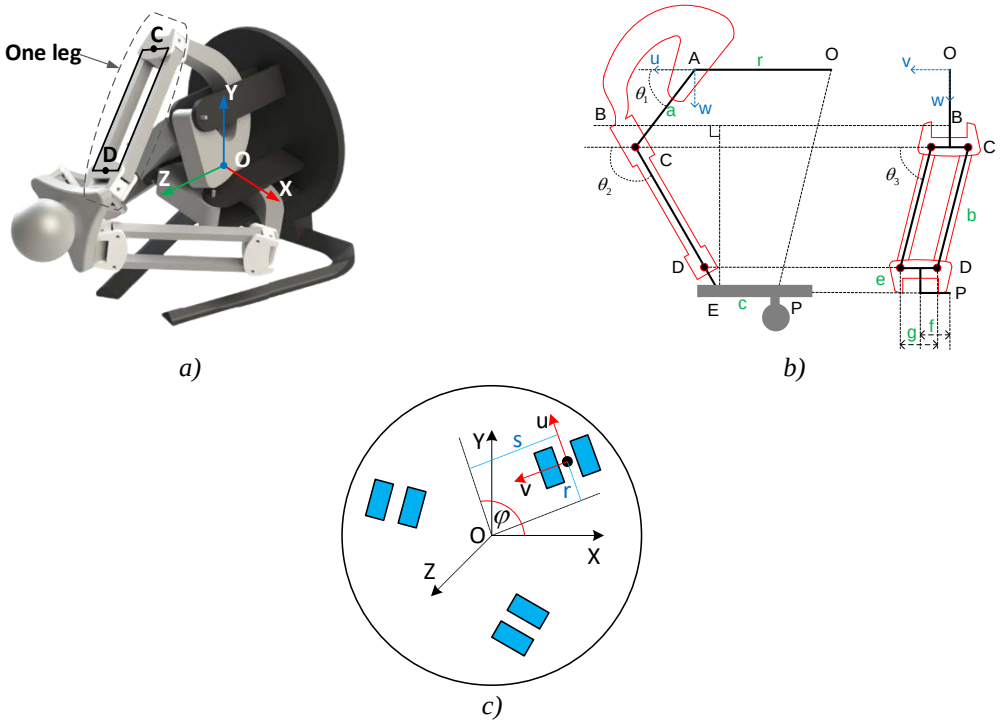

Figure 2. *The haptic model a) CAD model; b) side of view one leg; c) base*

The CAD model of the joystick is described in **Figure 2a**. The coordination of one leg is illustrated in **Figure 2b** and **Figure 2c**. O is the center of the original coordination on the XYZ axis, and P is the position of the end-effector of the haptic device. The UVW axis is attached to the base platform. θ_i is the angle at each joint of one leg (with $i = 1,2,3$), and the parameter of the haptic device is according to **Table 1**.

Table 1. *The parameter of the Novint Falcon haptic device*

Dimension	Value (mm)	Dimension	Value (mm)	Dimension	Value (mm)
a	**60**	**d**	**11.25**	**g**	**27.9**
b	**102.5**	**e**	**11.25**	**r**	**36.6**
c	**14.43**	**f**	**25**	**s**	**23.09**

After the end-effector's position is known, the inverse kinematic is calculated to determine each joint's angles. The transformation formula between the UVW and the XYZ is depicted as follows:

$$\overrightarrow{\mathbf{OP}} - \overrightarrow{\mathbf{OA}} = \begin{bmatrix} \cos\varphi_i & \sin\varphi_i & 0 \\ -\sin\varphi_i & \cos\varphi_i & 0 \\ 0 & 0 & 1 \end{bmatrix} \begin{bmatrix} P_x \\ P_y \\ P_z \end{bmatrix} - \begin{bmatrix} r \\ s \\ 0 \end{bmatrix} \tag{1}$$

where φ_1, φ_2, and φ_3 are the rotation angles with the value $7\pi/12$, $-\pi/12$, $-9\pi/12$.

Based on Figure 2, the vectors are described as follows:

$$\overrightarrow{\mathbf{OP}} - \overrightarrow{\mathbf{OA}} = \overrightarrow{\mathbf{AB}} + \overrightarrow{\mathbf{BE}} + \overrightarrow{\mathbf{EP}} \tag{2}$$

After calculating the vector $\overrightarrow{AB}$, $\overrightarrow{BE}$, $\overrightarrow{EP}$ and line segment BE, the result is as follows:

$$\overrightarrow{\mathbf{OP}} - \overrightarrow{\mathbf{OA}} = \begin{bmatrix} a\cos(\theta_1) \\ 0 \\ a\sin(\theta_1) \end{bmatrix} + \begin{bmatrix} \cos(\theta_2)\left(e+\sin(\theta_3)+d\right) \\ b\cos(\theta_3) \\ \sin(\theta_2)\left(e+b\sin(\theta_3)+d\right) \end{bmatrix} + \begin{bmatrix} -c \\ -f \\ 0 \end{bmatrix} \tag{3}$$

where $\overrightarrow{\mathbf{OP}} - \overrightarrow{\mathbf{OA}} = \overrightarrow{\mathbf{AP}} = \begin{bmatrix} P_u & P_v & P_w \end{bmatrix}^T$, the equation (3) is written as:

$$\begin{bmatrix} P_u \\ P_v \\ P_u \end{bmatrix} = \begin{bmatrix} a\cos(\theta_1)+\cos(\theta_2)\left(e+b\sin(\theta_3)+d\right)-c \\ b\cos(\theta_3)-f \\ a\sin(\theta_1)-\sin(\theta_2)\left(e+b\sin(\theta_3)+d\right) \end{bmatrix} \tag{4}$$

Thus, the θ_3 can be obtained by the following equation:

$$\theta_3 = \pm a\cos\left(\frac{P_v+f}{b}\right) \tag{5}$$

The results of the angle θ_1 can be demonstrated as follows:

$$\theta_1 = 2\tan^{-1}\left(\frac{B \pm \sqrt{B^2+A^2-C^2}}{A+C}\right) \tag{6}$$

where $A = 2\left(P_u+c\right)a$, $C = -\left(P_u+c\right)^2 - a^2 - P_w^2 - \left(e+b\sin(\theta_3)+d\right)^2$

After calculating the θ_3 and θ_1, the θ_2 angle is defined as:

$$\theta_2 = 2\tan^{-1}\left(\frac{P_w - a\sin(\theta_1)}{P_u+c-a\cos(\theta_1)}\right) \tag{7}$$

2.1.2. Forward kinematic of the haptic device

With the angles θ_1, θ_2 and θ_3 illustrated above, the forward kinematics for a 3-DOF parallel delta robot is solved. The structure of a 3-level parallel robot is described as follows:

a) *b)*

Figure 3. *The 3-level parallel robot a) constructor; b) description of the method of the intersection of 3 spheres*

JTE
HCMUTE
ISSN: 2615-9740

JOURNAL OF TECHNICAL EDUCATION SCIENCE
Ho Chi Minh City University of Technology and Education
Website: https://jte.edu.vn
Email: jte@hcmute.edu.vn

where θ_i is the deflection angle at the joints on the base plane, the point at the linked joints, and the point lying on the plane of the fixed base (i = 1, 2, 3). The method is described as follows: from the value of the angle θ_i, it is easy to calculate the coordinates at the points J_i. Furthermore, the center of the sphere J_i is chosen with a corresponding radius J_iE_i. If the sphere is moved along a vector $\overrightarrow{E_iE_0}$, a new sphere is created, and the intersection of these three spheres gets the point coordinates E_0. The coordinates of the center sphere after shifting the axis are respective J_1, J_2 and J_3.

Considering the 3-arm system, the J point in the UVW is rotated to the XYZ axis.

$$\begin{bmatrix} J_{xi} \\ J_{yi} \\ J_{zi} \end{bmatrix} = \begin{bmatrix} \cos(\varphi_i) & -\sin(\varphi_i) & 0 \\ \sin(\varphi_i) & \cos(\varphi_i) & 0 \\ 0 & 0 & 1 \end{bmatrix} \begin{bmatrix} J_{ui} - r \\ J_{vi} + s \\ J_{wi} \end{bmatrix} \tag{8}$$

With i = 1, 2, 3, the equation of the sphere with the three centers is found:

$$\begin{cases} (x - J_{x1})^2 + (y - J_{y1})^2 + (z - J_{z1})^2 = BE^2 \\ (x - J_{x2})^2 + (y - J_{y2})^2 + (z - J_{z2})^2 = BE^2 \\ (x - J_{x3})^2 + (y - J_{y3})^2 + (z - J_{z3})^2 = BE^2 \end{cases} \tag{9}$$

The position of the haptic device in terms of the x, y, and z axes relative to the Polar Coordinate System of robotics is known when solving the equation (9).

2.2. Kinematic of the 3-DOF robot

The 3-DOF coordination of the manipulator is depicted in **Figure 4**.

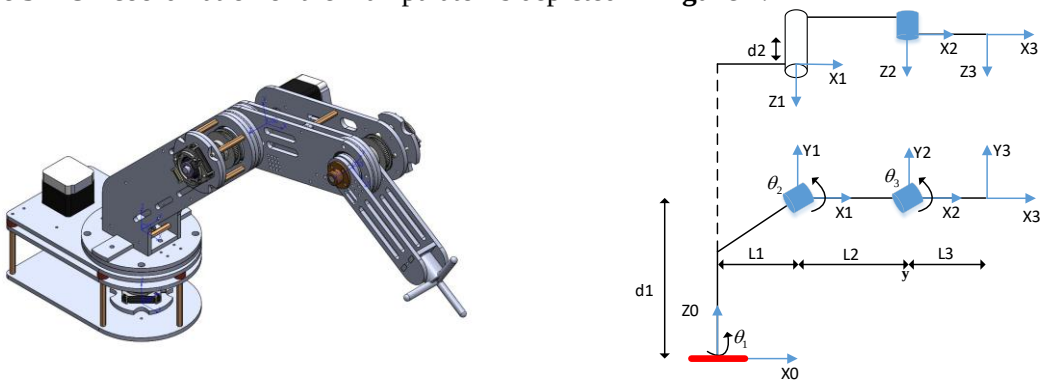

a) *b)*

Figure 4. *The coordinate system of the robot a) 3D model; b) description*

2.2.1. Forward kinematics of the manipulator

The kinematics of the robot are resolved by utilizing the Denavit-Hartenberg method. The D-H table can be illustrated as shown in **Table 2**.

Table 2. *The D-H table*

i	a_{i-1} (mm)	α_{i-1} (degrees)	d_i (mm)	θ_i (degrees)
1	L_1	90	d_1	θ_1
2	L_2	0	d_2	θ_2
3	L_3	0	0	θ_3

The translation matrix from the i axis to $i-1$ the axis [19] is as follows:

$$T_i^{i-1}=\begin{bmatrix}\cos(\theta_i) & -\sin(\theta_i)\cos(\alpha_i) & \sin(\theta_i)\sin(\alpha_i) & a_i\cos(\theta_i)\\ \sin(\theta_i) & \cos(\theta_i)\cos(\alpha_i) & -\cos(\theta_i)\sin(\alpha_i) & a_i\sin(\theta_i)\\ 0 & \sin(\alpha_i) & \cos(\alpha_i) & d_i\\ 0 & 0 & 0 & 1\end{bmatrix} \tag{10}$$

Then, the position of the robot is shown in the equation below:

$$\begin{cases}P_x=L_1c_1-d_2s_1+L_2c_1c_2+L_3c_1c_2c_3-L_3c_1s_2s_3\\ P_y=L_1s_1+d_2c_1+L_2c_2s_1+L_3c_2c_3s_1-L_3s_1s_2s_3\\ P_z=d_1+L_3s_{23}+L_2s_2\end{cases} \tag{11}$$

where $c_i=\cos(\theta_i)$, $s_i=sin(\theta_i)$, $s_{23}=\sin(\theta_2+\theta_3)$, with $i=1,2,3$.

2.2.2. Inverse kinematics of the manipulator

In the inverse kinematic problem, the position end effector in the XYZ axis is known. When resolving the inverse, the results are in the three joints of the robot.

The value of θ_1 can be determined as the equation (12):

$$P_xs_1-P_yc_1=-d_2 \tag{12}$$

The θ_1 angle is defined after solving the formula (12):

$$\theta_1=\text{atan2}\left(\pm\sqrt{1-\left(\frac{d_2}{\sqrt{P_x^2+P_y^2}}\right)^2},\frac{d_2}{\sqrt{P_x^2+P_y^2}}\right)-\alpha \tag{13}$$

when $\alpha=a\tan\left(\frac{P_x}{\sqrt{P_x^2+P_y^2}},\frac{P_y}{\sqrt{P_x^2+P_y^2}}\right)$.

The θ_2 angle is calculated as:

$$\begin{cases}P_xc_1+P_ys_1-L_1=L_2c_2+L_3c_{23}\\ P_z-d_1=L_2s_2+L_3s_{23}\end{cases} \tag{14}$$

Then, the θ_2 angle is defined as follows:

$$\theta_2=\text{atan2}\left(\frac{u^2+v^2+L_2^2-L_3^2}{\sqrt{(2uL_2)^2+(2vL_2)^2}},\pm\sqrt{1-\left(\frac{u^2+v^2+L_2^2-L_3^2}{\sqrt{(2uL_2)^2+(2vL_2)^2}}\right)^2}\right)-\beta \tag{15}$$

where $u=P_xc_1+P_ys_1-L_1$, $v=P_z-d_1$ and $\beta=a\tan 2\left(\frac{2uL_2}{\sqrt{(2uL_2)^2+(2vL_2)^2}},\frac{2vL_2}{\sqrt{(2uL_2)^2+(2vL_2)^2}}\right)$

Finally, the θ_3 angle is following the equation below:

$$\theta_3=\text{atan2}(v-L_2s_2,u-L_2c_2)-\theta_2 \tag{16}$$

3. Position Mapping and the Haptic Feedback method

3.1. Position Mapping Method

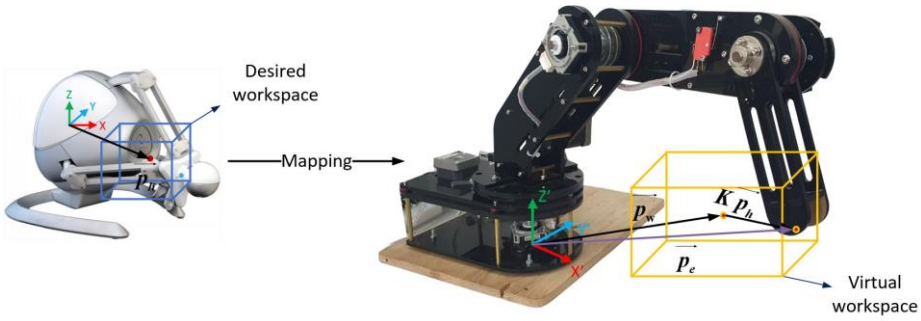

Figure 5. *The origin coordinate system of the Novint Falcon and the 3-DOF manipulator*

The position mapping method does not directly map two workspaces to each other but through selecting parameters to select the compatible slave and master workspace. Firstly, the joystick's workspace is identified based on its structure and joint limits. Then, a desired workspace is chosen based on the joystick's workspace. The workspace can either be in the shape of a cube that intersects with the joystick workspace or the entire joystick workspace. The desired workspace includes all positions converted to the setpoint of the 3-DOF manipulator using the position mapping algorithm. After that, the desired workspace is placed within the 3-DOF manipulator's workspace based on the $\mathbf{p}_w$ parameter, which is the translation vector of the joystick' workspace to the manipulator's workspace. Finally, the size of the desired workspace in the 3-DOF manipulator's workspace is adjusted based on the $\mathbf{K}$ parameter. This method is illustrated in **Figure 5**.

With the application of the Position mapping technique, the end-effector position of the slave robot is specified using the relation [20]:

$$\mathbf{p}_e = \mathbf{K}\mathbf{p}_h + \mathbf{p}_w \tag{17}$$

where $\mathbf{p}_e \in \Re^{3\times1}$ is the end effector's position of the 3-DOF manipulator relative to the original coordinate system $x'y'z'$, $\mathbf{p}_h \in R^{3\times1}$ is the end effector's position of the Novint Falcon relative to the axis system xyz viewed within the selected workbox, $\mathbf{p}_w \in R^{3\times1}$ is the center position of virtual workspace in the 3-DOF manipulator workspace relative to the coordinate system $x'y'z'$ and $\mathbf{K} \in \Re^{3\times3}$ is the scaling factor.

3.2. The Haptic Feedback Method

The haptic method assists the operator in controlling the robot during tasks and prevents it from entering the singularity area. When the robot reaches this area, a force is generated and transmitted to the operator's palm, providing sensory feedback and helping the operator remind the safety limitations.

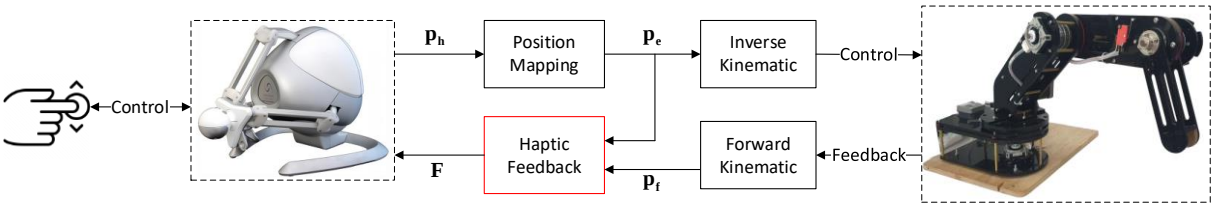

Figure 6. *Overview of the haptic system*

Figure 6 demonstrates the haptic feedback method. The joystick's position $\mathbf{p}_h$ is collected and converted to the desired position of the manipulator $\mathbf{p}_e$. The stepper motors in the actuators ensure the joint angle's response accuracy. The manipulator's position $\mathbf{p}_h$ is calculated using the forward kinematics formula. Finally, the force feedback is generated based on the displacement of $\mathbf{p}_e$ and $\mathbf{p}_h$.

The force feedback creates a sensation like stretching a tension spring. When a tension spring is stretched to an external force, it shrinks and offers resistance in the opposite direction. Based on Hooke's law, a virtual spring is simulated to provide force feedback. In addition, a damper is added to regulate the damping. The force feedback rendering is illustrated in **Figure 7**.

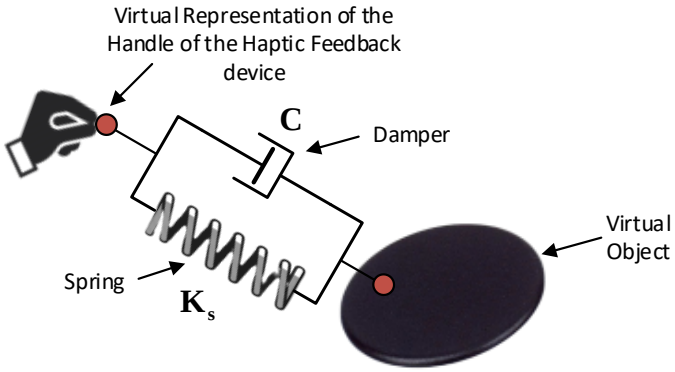

Figure 7. *Description of the haptic method*

The force feedback modeling is denoted as follows:

$$\mathbf{f} = \mathbf{K}_s \Delta\mathbf{x} + \mathbf{C}\mathbf{v} \tag{18}$$

where $\mathbf{f} \in \Re^{3\times1}$ is a force, $\mathbf{K}_s \in \Re^{3\times3}$ is the spring stiffness, $\Delta\mathbf{x} \in \Re^{3\times1}$ is the deformation, $\mathbf{C} \in \Re^{3\times3}$ is the damping coefficient, $\mathbf{v} \in \Re^{3\times1}$ is the velocity of the spring's deformation.

4. The experiment

This section presents the experiments to evaluate the effectiveness of the position mapping method in unifying the workspace of two robots and the meaning of the haptic feedback method when the haptic device is moved out of the desired workspace. A survey is conducted to select a suitable parameter for the position mapping algorithm. Then, the haptic feedback method experiments with the parameters of position mapping above are conducted.

4.1. Survey the appropriate parameters for the position mapping method

Step 1: To build the teleoperation system, the workspace of the robot and the haptic device is defined from the limited angle of each joint. The limited angles of the manipulator can be defined as: $\theta_1 \in [-110°, +75°]$, $\theta_2 \in [-110°, +120°]$, $\theta_3 \in [-120°, +110°]$. Besides, the limited angles of the haptic device are defined as: $\theta_i\,(i = 1,2,3) \in [-45°, +45°]$. The workspaces of the joystick and the 3-DOF manipulator are described in **Figure 8**.

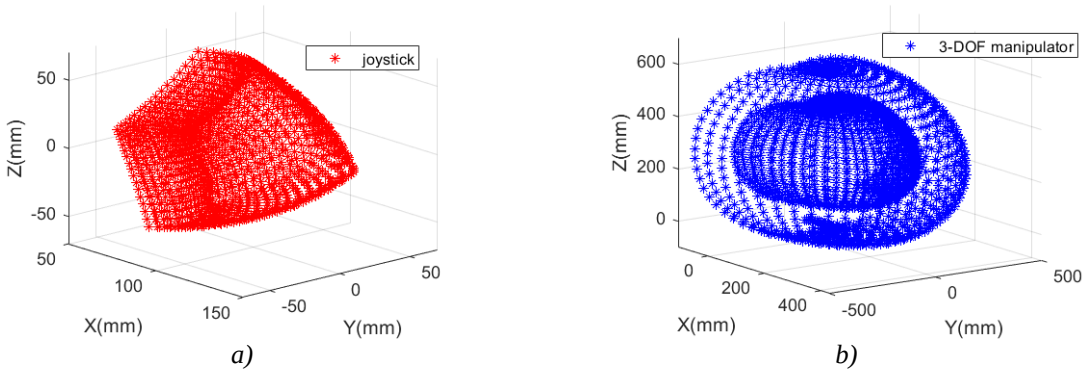

Figure 8. *The workspace of the a) joystick Novint Falcon; b) the 3-DOF manipulator*

Step 2: This step aims to determine the appropriate parameters of the position mapping method. Cases of this survey are listed in **Table 3**.

Table 3. *The survey of the parameters of the position mapping method*

Case	**K**	$\mathbf{p}_w$
1	$diag([1.3 \quad 3 \quad 2.5])$	$[0 \quad 0 \quad 205]^T$
2		$[90 \quad 0 \quad 205]^T$
3		$[500 \quad 0 \quad 205]^T$
4	$diag([2.6 \quad 6 \quad 3])$	$[0 \quad 0 \quad 205]^T$
5		$[90 \quad 0 \quad 205]^T$
6		$[500 \quad 0 \quad 205]^T$

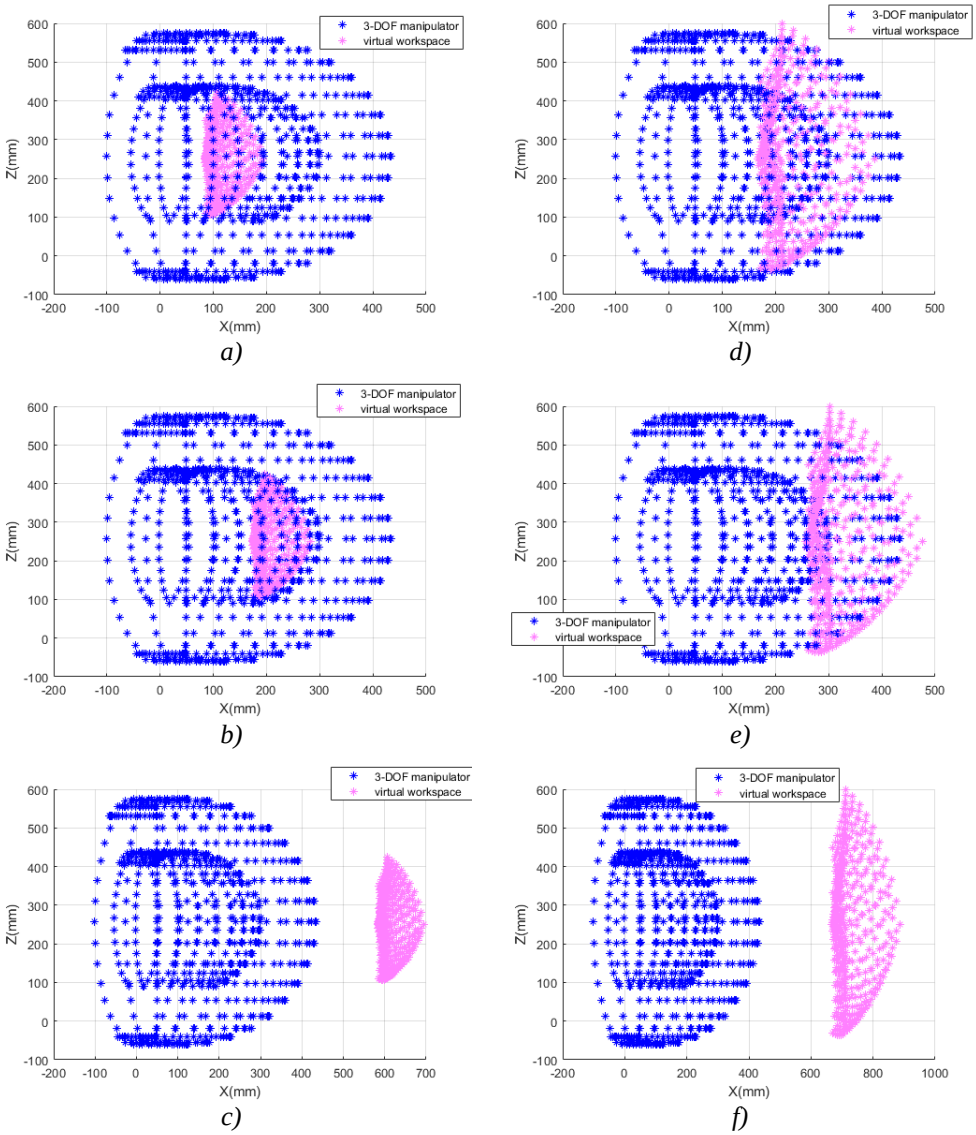

Figure 9. *The virtual workspace in the manipulator's workspace a) case 1; b) case 2; c) case 3; d) case 4; e) case 5; f) case 6*

JTE HCMUTE
ISSN: 2615-9740
JOURNAL OF TECHNICAL EDUCATION SCIENCE
Ho Chi Minh City University of Technology and Education
Website: https://jte.edu.vn
Email: jte@hcmute.edu.vn

The value of the scaling factor **K** is adjusted to change the shape of the desired workspace and makes the two unified workspaces more effective. The value of the translation vector $\mathbf{p}_w$ is adjusted to change the position of the virtual workspace in the manipulator's workspace. The results of the survey are shown in **Figure 9**. The workspace mapping method works best when the virtual workspace and the manipulator's workspace intersect as much as possible. As a result, the parameters in case 5 have achieved this. In this case, the singularity is solved by the haptic feedback method.

4.2. The experiment of the haptic-teleoperation system with the position mapping method

In this experiment, the teleoperation system is combined with the force feedback to advantage the operator's feeling about the environment. The new reflectance coefficient is selected to expand the working space. The parameter is following as: $\mathbf{K} = diag\left(\begin{bmatrix}2.6 & 6 & 5\end{bmatrix}\right)$; $\mathbf{p}_w = \begin{bmatrix}90 & 0 & 250\end{bmatrix}^T$.

In order to prevent the slave robot from being moved out of the designated workspace, the singularity area is designed to create an unstable system. The haptic method generates a force that acts against the direction of motion. During the experiment, the operator held the end effector of the haptic device and moved it out of the desired workspace, then returned it to the workspace. When the haptic device enters the singularity area, a force is applied to the palm of the operator's hand, which allows them to stop and reverse the movement of the end effector of the haptic device.

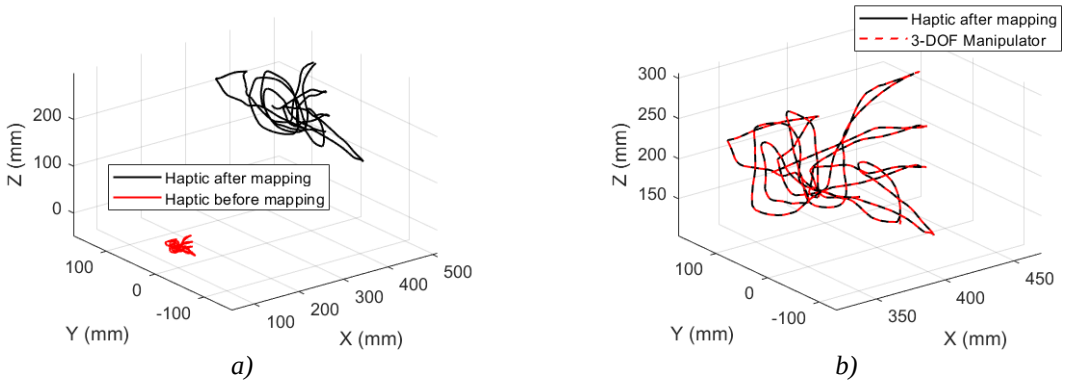

Figure 10. *The signals of the robot with the force feedback a) the haptic device; b) the robot arm*

The trajectory of the haptic device and the response of the 3-DOF manipulator is presented in **Figure 10**. The solid red line is the desired planning of the haptic device when the operator performs, the solid black line is the reference after using the mapping method, and the dashed red line is the position of the slave robot. The results show the effectiveness of the Position mapping method. The 3-DOF manipulator follows the setpoint from the haptic device and is not unstable, while the Novint Falcon device is out of the permitted spaces. The position of points outside the workspace of the 3-DOF robot is depicted in **Figure 11**.

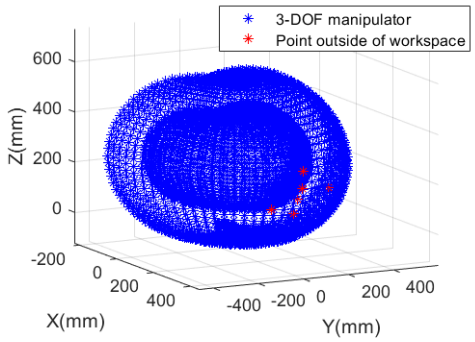

Figure 11. *The position of points located outside the workspace of the 3-DOF manipulator*

To evaluate the effectiveness of the position mapping and haptic method, **Figure 12** illustrates the system's responses to the position.

JTE
HCMUTE
ISSN: 2615-9740

JOURNAL OF TECHNICAL EDUCATION SCIENCE
Ho Chi Minh City University of Technology and Education
Website: https://jte.edu.vn
Email: jte@hcmute.edu.vn

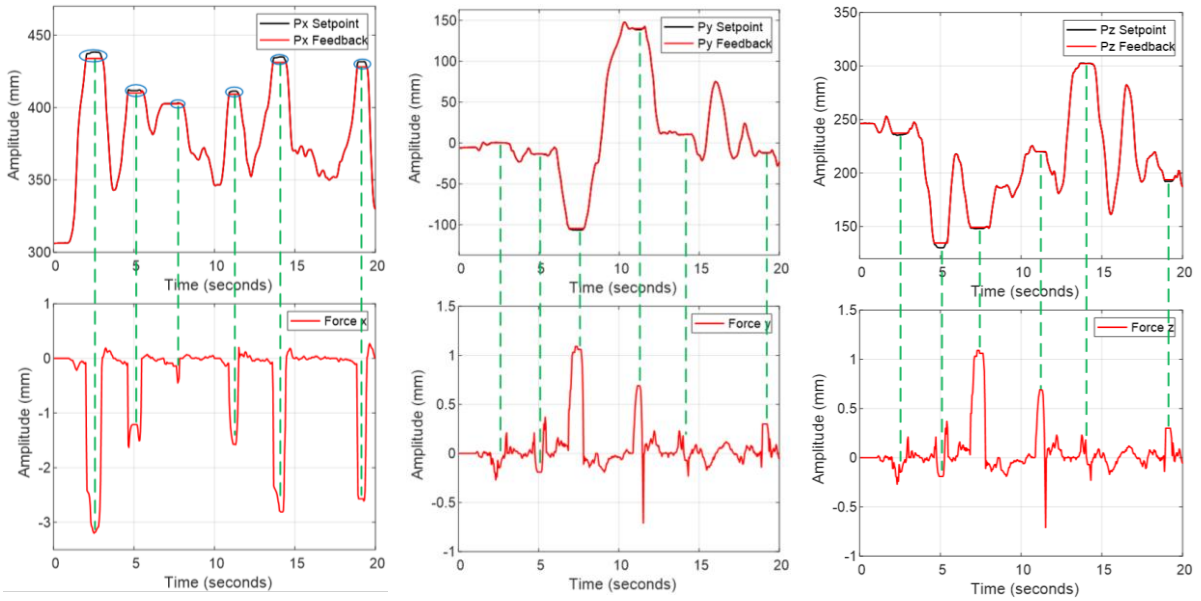

a) *b)* *c)*

Figure 12. *The response of the 3-DOF manipulator and the force feedback a) x-axis; b) y-axis; c) z-axis*

Based on **Figure 12**, the solid black is the setpoint from the haptic device after applying the position mapping method, the solid red line above is the measurement position of the 3-DOF manipulator, and the solid red line below is the generated force of the haptic device. At the singularity region, marked by the blue circle, the error of the position is more significant than the allowable threshold, but the response of the manipulator is still stable. The force value changes rapidly, and its direction is opposite to that of the force applied by the operator on the joystick. This force impacts the palm to alert the operator that the system has reached the limited workspace and helps the operator recognize the issue and return to the safety area.

5. Conclusions

This paper presented the mapping haptic method to unify two workspaces for the robot arm on the teleoperation system. The teleoperation system, including the 3-DOF manipulator and Novint Falcon haptic device, was established with Zigbee wireless communication. The Novin Falcon haptic device belongs to the master module, and the 3-DOF manipulator stays in the slave module. The operator moves the end-effector to generate the command for the 3-DOF manipulator. Because the workspaces of the falcon device and 3-DOF manipulator are different, the proposed method was developed with a position mapping algorithm to unify the workspace of the master-slave robots and a haptic feedback algorithm in the master robot to prevent the singularity in the slave robot. To verify the effectiveness of the proposed method, the proposed methods were applied to the experimental test bench. Using force feedback in the proposed method has helped to expand the entire workspace of the master device into the workspace of the slave device.

Acknowledgments

This research was studied at the Robotics and Intelligent Control Laboratory (RIC Lab), Faculty of Electrical and Electronics Engineering, Ho Chi Minh City University of Technology and Education, Vietnam.

Conflict of Interest

The authors declare no conflict of interest.

Data Availability Statement

The data that support the findings of this study are available from the corresponding author upon reasonable request.

REFERENCES

[1] R. Raj and A. Kos, "A Comprehensive Study of Mobile Robot: History, Developments, Applications, and Future Research Perspectives," *Applied Sciences*, vol. 12, no. 14, p. 6951, 2022.
[2] R. Saltaren, A. R. Barroso, and O. Yakrangi, "Robotics for Seabed Teleoperation: Part-1–Conception and Practical Implementation of a Hybrid Seabed Robot," *IEEE Access*, vol. 6, pp. 60559-60569, 2018.
[3] M. Panzirsch, R. Balachandran, B. Weber, M. Ferre, and J. Artigas, "Haptic Augmentation for Teleoperation through Virtual Grasping Points," *IEEE Trans Haptics*, vol. 11, no. 3, pp. 400-416, 2018.
[4] T. Fong, J. R. Zumbado, N. Currie, A. Mishkin, and D. L. Akin, "Space telerobotics: unique challenges to human–robot collaboration in space," *Reviews of Human Factors and Ergonomics*, vol. 9, no. 1, pp. 6-56, 2013.
[5] M. Shahbazi, S. F. Atashzar, and R. Patel, "A Systematic Review of Multilateral Teleoperation Systems," *IEEE Trans Haptics*, vol. 11, no. 3, pp. 338-356, 2018.
[6] J. Z. Y. Chen, C. Yang, B. Niu, "The workspace mapping with deficient-DOF space for the PUMA 560 robot and its exoskeleton arm by using orthogonal experiment design method," *Robotics and Computer-Integrated Manufacturing*, vol. 23, no. 4, pp. 478-487, 2007.
[7] A. Khalifa, A. Ramadan, K. Ibrahim, M. Fanni, S. Assal, and A. A. Ismail, "Workspace mapping and control of a teleoperated endoscopic surgical robot," in *19th International Conference on Methods and Models in Automation and Robotics (MMAR)*, 2014: IEEE, pp. 675-680.
[8] A. R. A. Khalifa, K. Ibrahim, M. Fanni, S. Assalz and A. A. Ismailk, "Workspace Mapping and Control of a Teleoperated Endoscopic Surgical Robot," in *19th International Conference on Methods and Models in Automation and Robotics (MMAR)*, Miedzyzdroje, Poland, 2014, pp. 675-680, doi: 10.1109/MMAR.2014.6957435.
[9] X. Gao, J. Silvério, E. Pignat, S. Calinon, M. Li, and X. Xiao, "Motion mappings for continuous bilateral teleoperation," *IEEE Robotics and Automation Letters*, vol. 6, no. 3, pp. 5048-5055, 2021.
[10] G. Liu, X. Geng, L. Liu, and Y. Wang, "Haptic based teleoperation with master-slave motion mapping and haptic rendering for space exploration," *Chinese Journal of Aeronautics*, vol. 32, no. 3, pp. 723-736, 2019.
[11] L. Liu, G. Liu, Y. Zhang, and D. Wang, "A modified motion mapping method for haptic device based space teleoperation," in *The 23rd IEEE International Symposium on Robot and Human Interactive Communication*, 2014: IEEE, pp. 449-453.
[12] H. V. A. Truong, D. T. Tran, X. D. To, K. K. Ahn, and M. Jin, "Adaptive fuzzy backstepping sliding mode control for a 3-DOF hydraulic manipulator with nonlinear disturbance observer for large payload variation," *Applied Sciences*, vol. 9, no. 16, p. 3290, 2019.
[13] H. V. A. Truong, D. T. Tran, and K. K. Ahn, "A neural network based sliding mode control for tracking performance with parameters variation of a 3-DOF manipulator," *Applied Sciences*, vol. 9, no. 10, p. 2023, 2019.
[14] G. S. Giri, Y. Maddahi, and K. Zareinia, "An application-based review of haptics technology," *Robotics*, vol. 10, no. 1, p. 29, 2021.
[15] Z. Ju, C. Yang, Z. Li, L. Cheng, and H. Ma, "Teleoperation of Humanoid Baxter Robot Using Haptic Feedback," in *International Conference on Multisensor Fusion and Information Integration for Intelligent Systems (MFI)*, Beijing, China, 2014, pp. 1-6, doi: 10.1109/MFI.2014.6997721.
[16] G. S. Giri, Y. Maddahi, and K. Zareinia, "An Application-Based Review of Haptics Technology," *Robotics*, 2021, doi: 10.3390/robotics10010029.
[17] N. Karbasizadeh, M. Zarei, A. Aflakian, M. Tale Masouleh, and A. Kalhor, "Experimental dynamic identification and model feed-forward control of Novint Falcon haptic device," *Mechatronics*, vol. 51, pp. 19-30, 2018.
[18] F. Khadivar, S. Sadeghnejad, H. Moradi, G. Vossoughi, and F. Farahmand, "Dynamic characterization of a parallel haptic device for application as an actuator in a surgery simulator," in *5th RSI international conference on robotics and mechatronics (ICRoM)*, 2017: IEEE, pp. 186-191.
[19] T. D. Hoa, N. V. Khiem, and T. D. Thien, "Design, simulate, fabricate, and control a 3-degree-of-freedom robotic arm," (in Vietnamese), *Journal of Technical Education Science*, no. 64, pp. 40-47, 2021.
[20] N. M. Chiedu and K. H. Zaad, "A hybrid position–rate teleoperation system," *Robotics and Autonomous Systems*, vol. 141, p. 103781, 2021.

Nguyen Tien Dat is currently studying in the Faculty For High-Quality Training, Ho Chi Minh University of Technology and Education, Vietnam, in 2023.
He works as a Robotics and Intelligent Control Lab member in the Department of Automation Control, Ho Chi Minh University of Technology and Education, Vietnam.
His research interests include robotics, cable robot, intelligent control and motion control.
Email: tiendat732001@gmail.com

Ly Phi Cuong is currently studying in the Faculty For High-Quality Training, Ho Chi Minh University of Technology and Education, Vietnam, in 2023.
He works as a Robotics and Intelligent Control Lab member in the Department of Automation Control, Ho Chi Minh University of Technology and Education, Vietnam.
His research interests include robotics, cable robot, intelligent control and motion control.
Email: lyphicuong2509@gmail.com

Tran Minh Khiem is currently studying in the Faculty For High-Quality Training, Ho Chi Minh University of Technology and Education, Vietnam, in 2023
He works as a Robotics and Intelligent Control Lab member in the Department of Automation Control, Ho Chi Minh University of Technology and Education, Vietnam.
His research interests include robotics, cable robot, intelligent control and motion control.
Email: minkeii@outlook.com

Tran Duc Thien received the B.S and M.S. degrees in the Department of Electrical Engineering Ho Chi Minh City University of Technology, Vietnam, in 2010, 2013, and the Ph.D. degree from University of Ulsan in 2020, respectively. He works as a lecturer with the Department of Automation Control, Ho Chi Minh City University of Technology and Education (HCMUTE), Vietnam. His research interests include robotics, variable stiffness system, fluid power control, disturbance observer, nonlinear control, adaptive control, fault tolerant control and intelligent technique. Email: thientd@hcmute.edu.vn. ORCID: https://orcid.org/0000-0002-6684-0681